J Nanostruct 15(2): 631-638, Spring 2025

RESEARCH PAPER

Design, Fabrication, and Characterization of N-Doped Decorated CeO_2 Composite for Degradation of Malachite Green

Suhad Kareem Abbas [1], Zainab M. Hassan [2], Faten Hadi Fakhri [3], Haithem Fadhil Abdulhasan [2], Wissam Abbas Ali [2]*

[1] *College of Applied Medical Science, University of Kerbala, Kerbala, Iraq*

[2] *Department of Chemistry, College of Science, University of Kerbala, Kerbala, Iraq*

[3] *Presidency University of Kerbala, Kerbala, Iraq*

ARTICLE INFO

Article History:
Received 27 January 2025
Accepted 20 March 2025
Published 01 April 2025

Keywords:
N-doped graphene quantum dots decorated CeO_2
Malachite green
Nanostructures
Photocatalyst
Pollutant

ABSTRACT

In this work, CeO_2 nanoparticles and N-doped GQDs decorated CeO_2 nanocomposites were synthesized through a hydrothermal process and characterized using various spectroscopy techniques, such as: Photoluminescence (PL), X-ray diffraction (XRD), ultraviolet and visible (UV-Vis), Fourier transform infrared (FT-IR), and field emission scanning electron microscopy (FE-SEM). The structural analysis confirmed the formation of N-doped GQDs and their integration into CeO_2, with various functional groups, for instance, hydroxyl, carbonyl, C=C, and C-N identified via FT-IR strategy. Optical characterization using ultraviolet-visible diffuse reflectance spectroscopy (DRS) showed that N-doped GQDs decorated CeO_2 composites exhibited a lower band gap (2.47 eV) compared to pure CeO_2 (2.63 eV), enabling enhanced photocatalytic performance under UV-Vis waves conditions. The nanocomposite demonstrated superior degradation efficiency of malachite green (94%), compared to CeO_2 alone (63%), due to band gap reduction and improved charge separation. Catalyst dosage optimization further confirmed that balanced loading enhances degradation efficiency. These findings highlight the potential of N-doped GQDs decorated CeO_2 nanocomposites for environmental remediation and photocatalytic wastewater treatment applications.

How to cite this article
Abbas S., Hassan Z., Fakhri F., Abdulhasan H., Ali W. Design, Fabrication, and Characterization of N-Doped Decorated CeO_2 Composite for Degradation of Methylene Blue. J Nanostruct, 2025; 15(2):631-638. DOI: 10.22052/JNS.2025.02.023

INTRODUCTION

When the poisonous materials enter water (*i.e.* oceans, seas, rivers, and lakes), water contamination occurs. These materials can dissolve in water or remain suspended on the surface of the water. The result of this issue is poor water quality. Water contamination occurs in various ways. In recent decades, water contamination is one of the most important industrial and environmental hazards and can be a concern for urbanization. Different sources, for instance, plastics, papers, and textile industries are generated these pollutants. [1-4]. Methylthioninium chloride, commonly named Methylene blue (MB), is an heteroaromatic dye that used more in industry. Because of the high toxicity and accumulations of this chemical in the

* *Corresponding Author Email: suhad.uokerbala@edu.iq*

environment, it has caused serious environmental problems. The recent studies presented that many researches have been performed to eliminate or separate of MB from water [5].

Graphene quantum dots have been introduced as a new member of nanocarbon structures. [6]. Based on recent reports, these nanocarbon structures have an excellent fluorescence [7, 8]. Besides, they reveal great biocompatibility [9], high cytotoxicity [10], high solubility in different solvents [11], can be graft with other structures via H-bonding [12]. Due to the wide availability of carbon sources, these properties hold promise for development in various applications: Fuel Cell, energy, sensors, and photocatalysts [13-15]. Doping is a smart approach to change optical and electrical properties of bulk semiconductor materials. The efficiency of GQD scaffolds can be easily optimized by doping agents: sulfur, nitrogen, and sulfur-nitrogen. Reports refer that the GQDs scaffolds doped with nitrogen have not large band gap. Furthermore, these structures show an absorption in the visible zone [16, 17]. Therefore, the range application of these scaffolds can be expanded in various fields: biosensors, photocatalyst, energy conversion, and biological imaging. [18, 19].

Among researchers, cerium(IV) oxide (CeO_2) is an appropriate case for photocatalytic performance, since it has unique 4f electrons, rich defect structures, great chemical stability, high oxygen storage capacity, and inexpensive price [20-22]. To the best of our knowledge, there are not many scientific papers available on GQDs-cerium oxide hybrids and their photocatalytic performance. Based on the mentioned background, it is a type of novel nanocarbon-based materials that contain oxygen, which can be beneficial for photocatalytic performance.

In this current paper, we introduced a facile and effective hydrothermal route to prepare nitrogen-doped graphene quantum dots by using citric acid 2-Hydroxypropane-1,2,3-tricarboxylic acid and ethylenediamine as carbon and nitrogen sources, respectively. In following, CeO_2/N-doped GQDs nanocomposites was prepared. The obtained compound has been confirmed by various spectroscopy techniques: PL, XRD, UV-Vis, FT-IR, and FE-SEM. The photocatalytic activity of products was finally investigated against malachite green under UV-Vis irradiation.

MATERIALS AND METHODS

Preparation of CeO_2 nanoparticles

According to previously method [23], $Ce(SO_4)_2.4H_2O$ was firstly dissolved in pure water (40 mL). Then, the alkaline solution (KOH, 5 *M*) was added. Also, the pH of medium was controlled by pH-meter set and reached 11. Next, the whole mixture was put to the autoclave system and kept under hydrothermal conditions (15h/ 140 °C). At completion, after filtering and washing, the obtained solid was dried at 50 °C. To give CeO_2 nanoparticles, the solid was finally calcined (120 minutes/ 600 °C).

General procedure of N-doped decorated CeO_2 nanocomposites preparation

Citric acid (1 g) was completely dissolved in 40 mL of pure H_2O and stirred for 3 min to form the transparent solution. After that, ethylenediamine (0.5 mL) was added and stirred again for 60 s at room temperature. Next, 1.5 g of as-prepared Ce_2O nanoparticles was added and stirred again for 5-6 min at room temperature. The mixture was then moved to autoclave and heated in an oven (12h/ 180 °C). The as-prepared CeO_2/N-doped GQDs nanocomposite was obtained, washed two times with dry C_2H_5OH, and dried in an oven.

Photocatalyst test

Under UV light waves, the photocatalytic performance of as-prepared N-doped decorated CeO_2 nanocomposites was studied by checking the degradation of methyl blue (MB) in a water media. Test condition included the use of UV lamp (400 W, Orsam model) located at a determined distance 0.2 meter away from the reaction medium. The as-synthesized dye solution (100 mL solution including the mixture of CeO_2 nanoparticles (0.1 g) or as-prepared N-doped decorated CeO_2 nanocomposites (0.1g), MB solution (10 ppm), and double-distilled water in neutral pH) was stirred (0.5 h) in a dark medium to get suitable balance of adsorption and desorption of the dye molecules on the surface of N-doped decorated CeO_2 nanocomposites, which is necessary for them to function effectively as a photocatalyst. The air was pumped into reaction medium to remain the solution oxygen-saturated all over the reaction. Next, the CeO_2 nanoparticles and N-doped decorated CeO_2 nanocomposites were separated from samples (6 mL), collected from the degraded solution at different times, and centrifuged at

12000 rpm (5 min). The concentration of dye was investigated by UV-Vis strategy.

RESULTS AND DISCUSSION

Ce_2O nanoparticles was prepared by hydrothermal process. The hydrothermal process was also applied for the synthesis of the dye molecules on the N-doped decorated CeO_2 nanocomposites [6]. The characterization of pure Ce_2O nanoparticles and the N-doped decorated

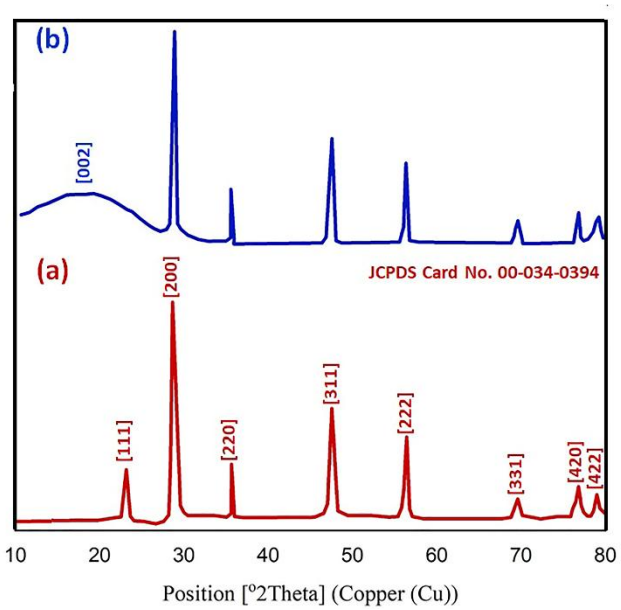

Fig. 1. XRD patterns of pure Ce_2O nanoparticles (a) and N-doped decorated CeO_2 nanocomposites (b).

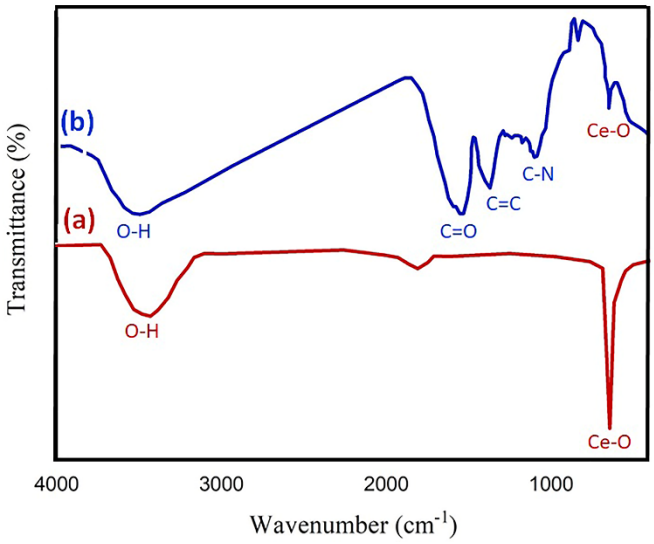

Fig. 2. The FT-IR curves of pure Ce_2O nanoparticles (a) and N-doped decorated CeO_2 nanocomposites (b).

CeO_2 nanocomposites were characterized by XRD method. The XRD results of pure Ce_2O nanoparticles and N-doped decorated CeO_2 nanocomposites were displayed in Fig. 1. From Fig. 1a, the all diffraction peaks were observed and this pattern matched with standard card (JCPDS Card No. 00-034-0394) [24]. Moreover, a broad peak is located at *2Theta*= 22° relating to the [002] plane cab corresponded to disordered structure of N-doped graphene quantum dots (Fig. 2a) [1].

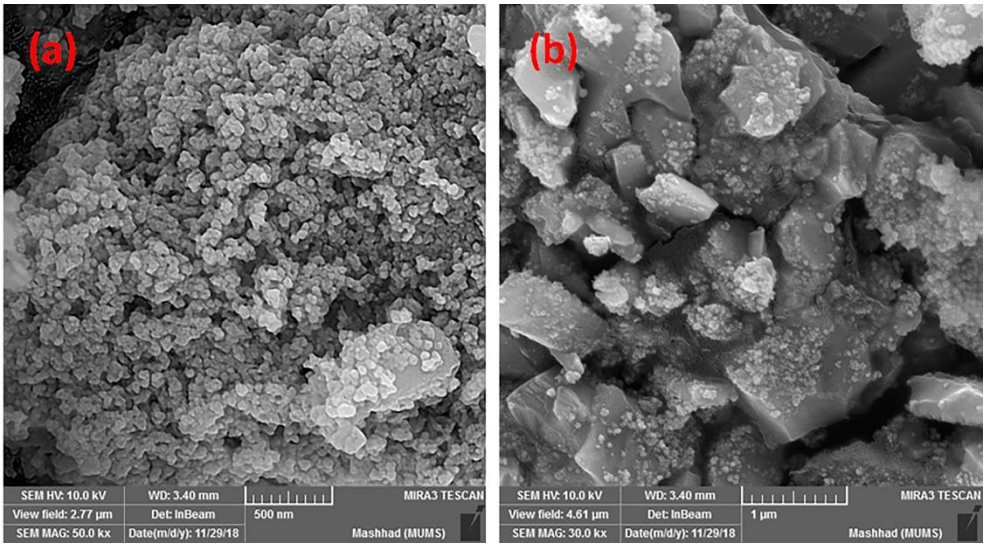

Fig. 3. FE-SEM images of pure CeO_2 nanoparticles (a) and N-doped decorated CeO_2 nanocomposites (b).

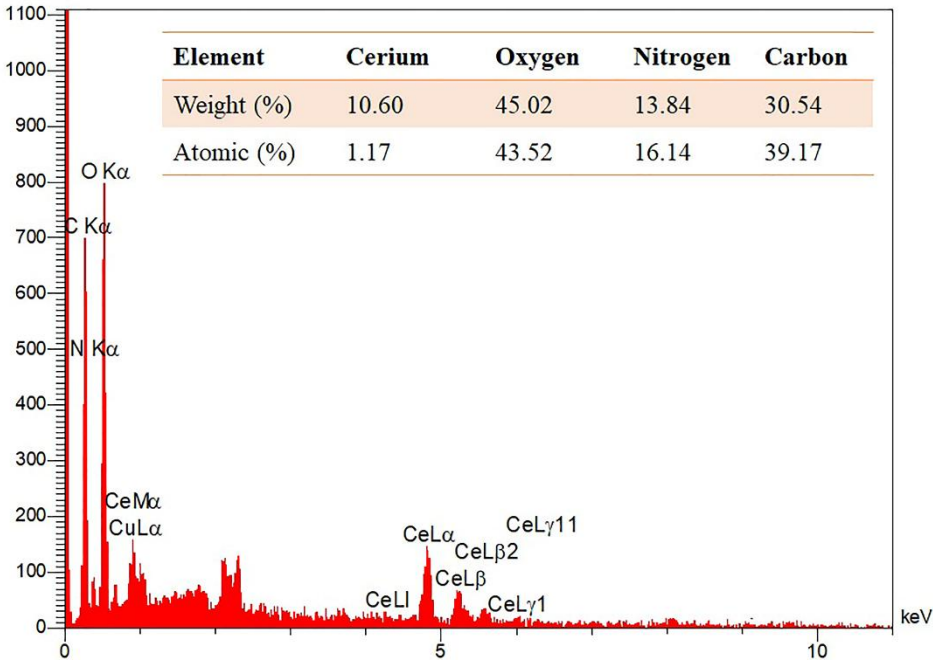

Fig. 4. EDX results of CeO_2/N-doped GQDs nanocomposites

The functional groups of surface were studied through FT-IR method. The FT-IR curve of pure Ce_2O nanoparticles and N-doped decorated CeO_2 nanocomposites were displayed in Fig. 2. According to Fig. 2a, the absorption bond at wavenumber of 3280 cm^{-1} is corresponded to the stretching absorption of hydroxyl group. The band is located at wavenumber of 665 cm^{-1} is related to Ce-O band [25, 26]. The presence of O-H (strong and broad peak), C=O, C=C, and C-N bands are seen at 3430, 1665, 1475-1575, and 1215 cm^{-1}, respectively [27]. These results confirmed the generation of the N-doped GQDs. In addition, data from FT-IR data display that the obtained compound includes N and COOH containing functional groups.

To study of the morphology and particles size of nanocomposites, FE-SEM analysis was used. The FE-SEM pictures of Ce_2O nanoparticles and N-doped decorated CeO_2 nanocomposites are shown in Fig. 3. Based on FE-SEM images, the average particles size of obtained nanostructures was reported 434 nm. In addition to FE-SEM analysis, EDX analysis was used for investigation of chemical composition. The EDX pattern confirmed the presence on cerium, oxygen, nitrogen, and carbon elements in the CeO_2/N-doped GQDs nanocomposites. The results of EDX analysis were displayed in Fig. 4.

The photocatalytic efficiency of a material is closely linked to its light absorption capability. Fig. 5a and Fig. 5c presents the ultraviolet-visible diffuse reflectance spectra (DRS) for CeO_2 and

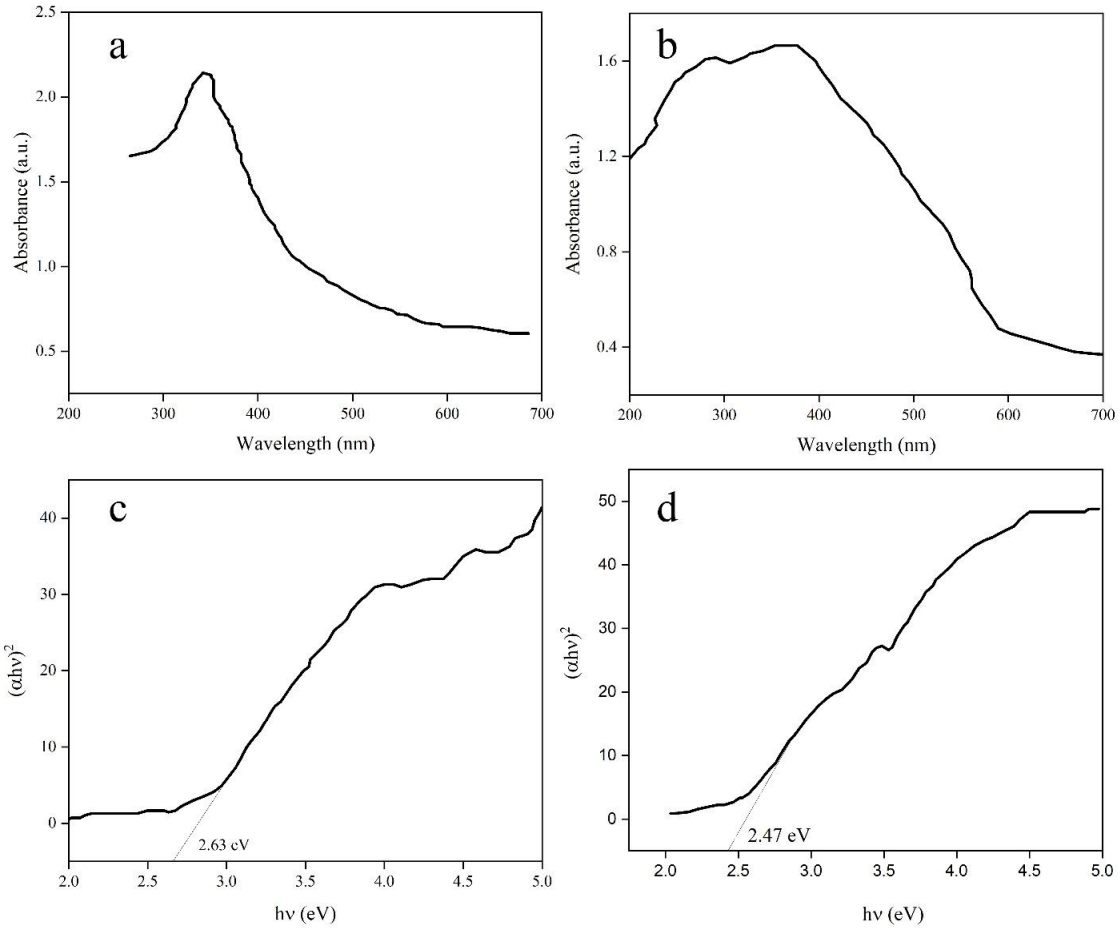

Fig. 5. a) UV-Vis curve of CeO_2 nanoparticles b) UV-Vis curve of N-doped decorated CeO_2 nanocomposites c) plot of $(\alpha hu)^2$ versus hu for measuring band gap of CeO_2 nanoparticles d) plot of $(\alpha hu)^2$ versus hu for measuring band gap of N-doped decorated CeO_2 nanocomposites.

the CeO_2/N-GQDs nanocomposite. To determine the most effective light source for initiating photocatalytic dye degradation, an understanding of the band gap is essential. The proposed band gap for pure CeO_2 and the N-doped decorated CeO_2 nanocomposites was assessed by comparing the $(ahυ)^n$ curve to zero hυ (Fig. 5b and Fig. 5d). Based on this tests, the estimated band gap of pure CeO_2 nanostructure was determined to be 2.63 eV. In contrast, the N-doped decorated CeO_2 nanocomposites exhibited a lower band gap of 2.47 eV, indicating that UV-Vis light irradiation is the most suitable source for photocatalytic activity. These findings confirm that N-GQDs and CeO_2 have been appropriately hybridized to establish a Z-scheme heterojunction, which enhances charge separation and improves photocatalytic efficiency.

Malachite green has been found to be moderately toxic and an extreme irritant. Studies indicate that it can intercalate with DNA, potentially leading to mutagenic effects. The photocatalytic degradation of malachite green was conducted to evaluate the functionality of the as-prepared photocatalysts. The initial tests were performed under controlled conditions, including a pH solution=7, a primary of malachite green: 6 mg/L, and a photocatalyst loading: 50 mg. The mixture was stirred in the dark medium for 0.5 h to achieve a balance of adsorption and desorption, with samples collected every 15 minutes to monitor the adsorption of malachite green before light exposure. Subsequently, the photoreactor was illuminated with UV-vis light. The photocatalytic performance of CeO_2 and the CeO_2/N-GQDs nanocomposite in terms of malachite green removal efficiency is depicted in Fig. 6. N-doped decorated CeO_2 nanocomposites achieved 94% removal (Fig. 6b), meanwhile, CeO_2 alone achieved 63% removal within the same timeframe (Fig. 6a). The improved photocatalytic performance of N-doped decorated CeO_2 nanocomposites compared to CeO_2 was attributed to band gap reduction and the establishment of a N-doped decorated CeO_2 nanocomposites.

The catalyst dosage has a crucial role in determining the rate of organic dye degradation in photocatalytic reactions. While increasing the catalyst quantity generally enhances degradation by providing more active regions for light absorption and the generation of reactive species, for instance: hydroxyl radicals (•OH). The catalyst acts as a reaction surface, facilitating the generation of reactive oxygen species (ROS) that break down malachite green [28]. A higher catalyst concentration accelerates degradation, but practical limitations must be considered when optimizing its amount. Excessive catalyst usage may lead to higher costs and complex recovery processes, while insufficient catalyst can result in partial oxidation of the dye or extended reaction times. Striking the right balance requires experimental validation to determine the most effective material concentration. In the conducted tests, photocatalytic efficiencies of 82%, 94%, and 89% were achieved with catalyst dosages of 3, 6 g, and 9 mg/L, respectively, for N-doped decorated

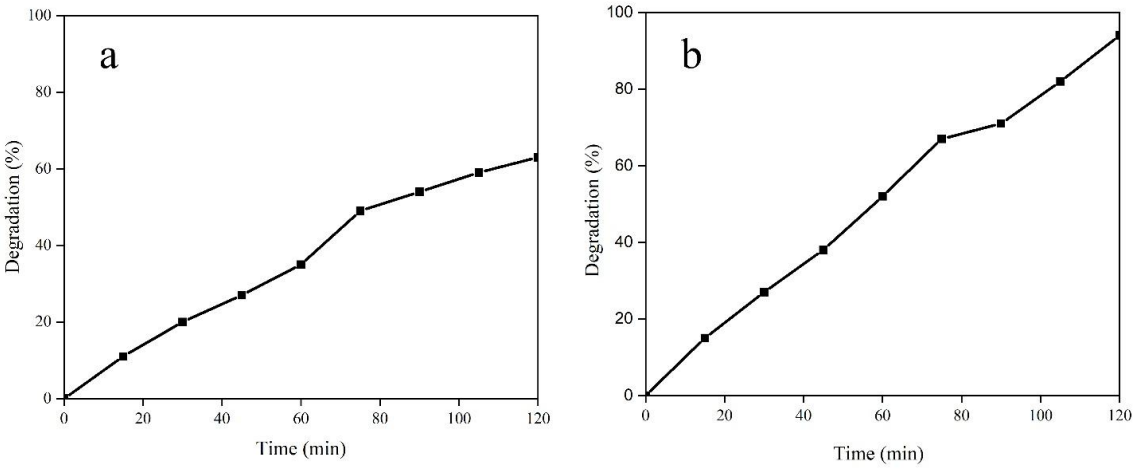

Fig. 6. Photocatalytic activity of a) CeO_2 nanoparticles b) CeO_2/N-GQDs nanocomposites.

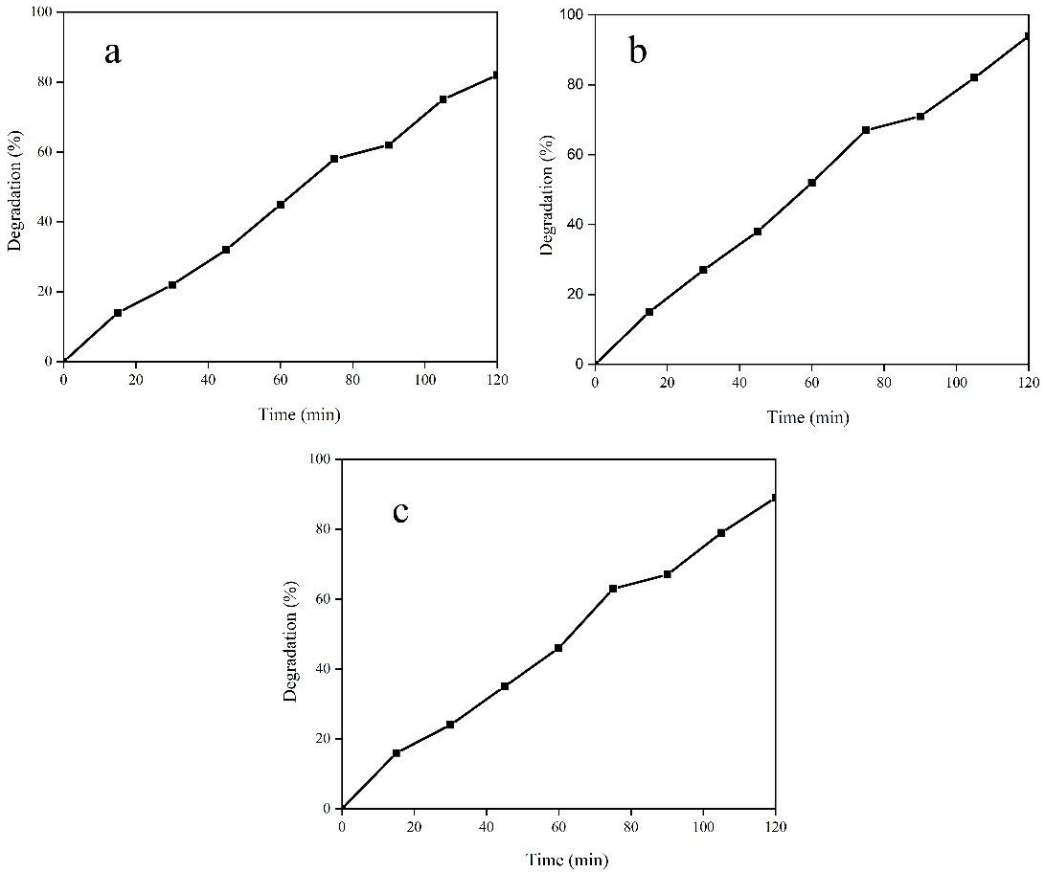

Fig. 7. Photocatalytic activity of a) 3 b) 6 c) 9 mg/L of N-doped decorated CeO_2 nanocomposites.

CeO_2 nanocomposites (Fig. 7). These findings underscore the importance of optimal catalyst loading, ensuring maximum dye degradation efficiency while maintaining economic feasibility and effective reaction control.

CONCLUSION

In this study, Ce_2O nanoparticles and N-doped decorated CeO_2 nanostructures were successfully fabricated through the hydrothermal route and comprehensively confirmed applying XRD, DRS, FT-IR, FE-SEM, and EDX analyses. Structural and functional investigations confirmed the incorporation of N-doped GQDs, leading to the formation of a Z-scheme heterojunction, which effectively enhances charge separation and photocatalytic activity. Band gap analysis revealed that the N-doped decorated CeO_2 nanostructures exhibited a lower band gap (2.47 eV) compared to pure CeO_2 (2.63 eV), indicating improved light absorption under UV-Vis irradiation. These findings validate the efficient hybridization of CeO_2 with N-GQDs, which extends the material's photocatalytic responsiveness and enhances its degradation capability. The photocatalytic functionality of the synthesized nanocatalyst was further assessed through the degradation of malachite green, a toxic organic dye with potential mutagenic effects. Under optimized conditions (pH 7, the primary concentration of dye: 6 mg/L, and 50 mg catalyst loading), the N-doped decorated CeO_2 nanocomposites achieved a superior degradation efficiency of 94%, significantly surpassing pure CeO_2 (63%). The enhanced performance was attributed to band gap reduction, increased charge separation yield, and the generation of reactive oxygen species (ROS). Furthermore, catalyst dosage optimization was explored to determine the most effective concentration for maximum dye degradation. Experimental results demonstrated that a balanced catalyst loading is essential to avoid excessive reagent costs and

unwanted charge recombination effects. The N-doped decorated CeO_2 nanostructures exhibited photocatalytic efficiencies of 82%, 94%, and 89% at catalyst dosages of 3, 6, and 9 mg/L, respectively, confirming the importance of dosage regulation in achieving optimal degradation performance.

CONFLICT OF INTEREST

The authors declare that there is no conflict of interests regarding the publication of this manuscript.

REFERENCE

1. Safardoust-Hojaghan H, Salavati-Niasari M. Degradation of methylene blue as a pollutant with N-doped graphene quantum dot/titanium dioxide nanocomposite. Journal of Cleaner Production. 2017;148:31-36.
2. Albayati TM, Sabri AA, Alazawi RA. Separation of Methylene Blue as Pollutant of Water by SBA-15 in a Fixed-Bed Column. Arabian Journal for Science and Engineering. 2015;41(7):2409-2415.
3. Alves LA, de Castro AH, de Mendonça FG, de Mesquita JP. Characterization of acid functional groups of carbon dots by nonlinear regression data fitting of potentiometric titration curves. Appl Surf Sci. 2016;370:486-495.
4. Ambika S, Sundrarajan M. Green biosynthesis of ZnO nanoparticles using Vitex negundo L. extract: Spectroscopic investigation of interaction between ZnO nanoparticles and human serum albumin. J Photochem Photobiol B: Biol. 2015;149:143-148.
5. Chin S, Park E, Kim M, Jurng J. Photocatalytic degradation of methylene blue with TiO_2 nanoparticles prepared by a thermal decomposition process. Powder Technol. 2010;201(2):171-176.
6. Safaei-Ghomi J, Bateni FS, Babaei P. CeO_2/CuO@N-GQDs@NH_2 nanocomposite as a high-performance catalyst for the synthesis of benzo[g]chromenes. Appl Organomet Chem. 2020;34(7).
7. Deming CP, Mercado R, Gadiraju V, Sweeney SW, Khan M, Chen S. Graphene Quantum Dots-Supported Palladium Nanoparticles for Efficient Electrocatalytic Reduction of Oxygen in Alkaline Media. ACS Sustainable Chemistry & Engineering. 2015;3(12):3315-3323.
8. Safaei-Ghomi J, Pooramiri P, Babaei P. Green sonosynthesis of phenazinpyrimidines using CO_3O_4@ZnO@N-GQDs@SO_3H nanocomposite as a robust heterogeneous catalyst. J Chin Chem Soc. 2021;68(7):1302-1309.
9. Derakhshan Z, Baghapour MA, Ranjbar M, Faramarzian M. Adsorption of Methylene Blue Dye from Aqueous Solutions by Modified Pumice Stone: Kinetics and Equilibrium Studies. Health Scope. 2013;2(3):136-144.
10. Guillén-Santiago A, Mayén SA, Torres-Delgado G, Castanedo-Pérez R, Maldonado A, Olvera MdlL. Photocatalytic degradation of methylene blue using undoped and Ag-doped TiO2 thin films deposited by a sol–gel process: Effect of the ageing time of the starting solution and the film thickness. Materials Science and Engineering: B. 2010;174(1-3):84-87.
11. Hao X, Jin Z, Xu J, Min S, Lu G. Functionalization of TiO_2 with graphene quantum dots for efficient photocatalytic hydrogen evolution. Superlattices Microstruct. 2016;94:237-244.
12. Hu C, Liu Y, Yang Y, Cui J, Huang Z, Wang Y, et al. One-step preparation of nitrogen-doped graphenequantum dots from oxidized debris of graphene oxide. J Mater Chem B. 2013;1(1):39-42.
13. Kang Y-F, Li Y-H, Fang Y-W, Xu Y, Wei X-M, Yin X-B. Carbon Quantum Dots for Zebrafish Fluorescence Imaging. Sci Rep. 2015;5:11835-11835.
14. Ke C-C, Yang Y-C, Tseng W-L. Synthesis of Blue-, Green-, Yellow-, and Red-Emitting Graphene-Quantum-Dot-Based Nanomaterials with Excitation-Independent Emission. Particle & Particle Systems Characterization. 2015;33(3):132-139.
15. Mohamed O, Abdel-Fattah A, Nadim M, Abdel-Bary T. The effect of bone anchored maxillary protraction on maxillary-mandibular divergency. Egyptian Orthodontic Journal. 2014;46(12):41-47.
16. Liang Q, Ma W, Shi Y, Li Z, Yang X. Easy synthesis of highly fluorescent carbon quantum dots from gelatin and their luminescent properties and applications. Carbon. 2013;60:421-428.
17. Mandani S, Sharma B, Dey D, Sarma TK. Carbon nanodots as ligand exchange probes in Au@C-dot nanobeacons for fluorescent turn-on detection of biothiols. Nanoscale. 2015;7(5):1802-1808.
18. Mohan SV, Karthikeyan J. Removal of lignin and tannin colour from aqueous solution by adsorption onto activated charcoal. Environ Pollut. 1997;97(1-2):183-187.
19. Murashkina AA, Murzin PD, Rudakova AV, Ryabchuk VK, Emeline AV, Bahnemann DW. Influence of the Dopant Concentration on the Photocatalytic Activity: Al-Doped TiO_2. The Journal of Physical Chemistry C. 2015;119(44):24695-24703.
20. Yan YQ, Wu YZ, Wu YH, Weng ZL, Liu SJ, Liu ZG, et al. Recent Advances of CeO_2-Based Composite Materials for Photocatalytic Applications. ChemSusChem. 2024;17(14).
21. Matussin SN, Harunsani MH, Khan MM. CeO_2 and CeO_2-based nanomaterials for photocatalytic, antioxidant and antimicrobial activities. Journal of Rare Earths. 2023;41(2):167-181.
22. Abad A, Concepción P, Corma A, García H. A Collaborative Effect between Gold and a Support Induces the Selective Oxidation of Alcohols. Angew Chem. 2005;117(26):4134-4137.
23. Baudin M, Wójcik M, Hermansson K. Dynamics, structure and energetics of the (111), (011) and (001) surfaces of ceria. Surface Science. 2000;468(1-3):51-61.
24. Shanmugam P, Kuppuswamy GP, Pushparaj K, Arumugam B, Sundaramurthy A, Sivalingam Y. CeO_2 nanoparticles based extended gate field effect transistor for enzyme free detection of glucose. Journal of Materials Science: Materials in Electronics. 2021;33(12):9483-9489.
25. Ramachandran M, Subadevi R, Sivakumar M. Role of pH on synthesis and characterization of cerium oxide (CeO_2) nano particles by modified co-precipitation method. Vacuum. 2019;161:220-224.
26. McDevitt NT, Baun WL. Infrared absorption study of metal oxides in the low frequency region (700-240 cm−1). Spectrochim Acta. 1964;20(5):799-808.
27. Babaei P, Safaei-Ghomi J. l-proline covered N doped graphene quantum dots modified CuO/ZnO hexagonal nanocomposite as a robust retrievable catalyst in synthesis of substituted chiral 2-amino-4H-chromenes. Materials Chemistry and Physics. 2021;267:124668.
28. Osanloo M, Khorasheh F, Larimi A. Fabrication of nano-dandelion magnetic TiO_2/$CuFe_2O_4$ doped with silver as a highly visible-light-responsive photocatalyst for degradation of Naproxen and Rhodamine B. J Mol Liq. 2024;407:125242.